#### Research Article

Heru Sukanto\*, Joko Triyono, Dody Ariawan, Muhammad Takbir Alfarisi, Wijang Wisnu Raharjo, Latifah Nur Hikmah and Rachmad Imbang Tritjahjono

# Micromechanic models for manufacturing quality prediction of cantula fiber-reinforced nHA/ magnesium/shellac as biomaterial composites

https://doi.org/10.1515/jmbm-2025-0066 received November 06, 2024; accepted May 12, 2025

Abstract: The novelty of this study lies in the integration of cantula fibers (CaFs), natural fibers known for their high mechanical strength and eco-friendly properties, into a biodegradable composite system (Mg/nHA/shellac) designed for potential biomedical applications, particularly bone screws. This research evaluates the tensile strength and elastic modulus of the composite through experimental testing and micromechanical modeling, establishing key benchmarks for assessing the biocomposite performance prior to further characterization. The significance of this work is underscored by the increasing need for sustainable and biodegradable biomaterials that can replace conventional implants, thereby reducing environmental impact while enhancing biocompatibility. Experimental findings demonstrate that the incorporation of CaFs significantly improves both the tensile strength and elastic modulus as the fiber content increases. Comparative analysis shows that the Bowyer-Bader model most accurately predicts the tensile strength, while the Cox-Krenchel model offers the best prediction for elastic modulus. However, discrepancies observed between theoretical and experimental results highlight the anisotropic nature of CaFs and the complex interactions within the composite matrix. These insights offer structural optimization efforts on natural fiber-reinforced biocomposites. The outcome of this study advances the development of cost-effective, environmentally sustainable biomaterials with enhanced mechanical performance for biomedical applications.

Joko Triyono, Dody Ariawan, Muhammad Takbir Alfarisi, Wijang Wisnu Raharjo, Latifah Nur Hikmah: Mechanical Engineering Department, Sebelas Maret University, Surakarta, Indonesia Rachmad Imbang Tritjahjono: Mechanical Engineering Department, Polytechnic of Bandung, Bandung, Indonesia

**Keywords:** cantula fiber, micromechanical analysis, tensile strength, nano-hydroxyapatite

#### 1 Introduction

Biomaterials that are biodegradable offer potential as primary constituents for medical implants aimed at supporting the healing process [1]. Magnesium and its alloys have garnered recent attention as metals in biomaterials due to their biocompatibility, mechanical properties, and biodegradability [2]. In addition, nano-hydroxyapatite (nHA), an inorganic compound constituting bones and teeth with the chemical formula  $\text{Ca}_{10}(\text{PO}_4)_6(\text{OH})_2$ , is also widely utilized in biomedical applications, particularly in orthopedics [3,4].

The bioadhesive binder between Mg and nHA is shellac, a natural polymer known for its environmentally friendly, non-toxic, renewable properties and ability to form waterproof layers. Shellac is considered a promising binder in the biomaterial industry, albeit its current minimal application [5]. To further enhance the mechanical properties of the composite, natural fibers such as Agave cantula Roxb. fiber (CaF) have been incorporated. Cantula fibers (CaFs) are recognized for their high mechanical strength, lightweight nature, durability, cost-effectiveness, and eco-friendliness. With a cellulose content of approximately 64.23%, CaF holds significant potential as a reinforcement material in composites [6]. Recent studies have demonstrated that natural fibers, when properly treated and integrated into polymer matrices, can significantly improve the tensile strength, stiffness, and fracture toughness [7]. For instance, the mechanical properties of natural fiber-reinforced composites are highly dependent on fiber orientation, interfacial adhesion, and the distribution of fibers within the matrix. These factors influence the stress transfer efficiency and the overall composite performance, making natural fibers a viable alternative to synthetic reinforcements in biocomposites.

<sup>\*</sup> Corresponding author: Heru Sukanto, Mechanical Engineering Department, Sebelas Maret University, Surakarta, Indonesia, e-mail: herusukanto@staff.uns.ac.id

2 — Heru Sukanto *et al.* DE GRUYTER

In order to streamline research time and reduce costs associated with experimental methods, predictions of tensile strength and elastic modulus were conducted using established mathematical models and numerical techniques for mechanical composites. Crucial to this approach is the consideration of intrinsic properties of fibers and the matrix essential for accurately predicting mechanical properties of the Mg/nHA/shellac composite mixture [8]. This study focuses specifically on two models renowned for accurately predicting tensile strength: the Hirsch model equation and the Bowyer-Bader model. For predicting elastic modulus, the Tsai-Pagano model, Cox-Krenchel model, Christensen model, Cox model, and Manera model equations were employed. These models were selected based on their extensive utilization and track record of reliable predictions in prior research studies [9]. Key to obtaining necessary data is the determination of interfacial shear stress (IFSS), which requires conducting a single pull-out fiber test [10].

This study aims to bridge the gap between experimental and theoretical approaches by evaluating the accuracy of micromechanical models in predicting the mechanical properties of Mg/nHA/shellac composites reinforced with CaFs. By integrating recent advancements in natural fiber-reinforced composites and micromechanical modeling, this work contributes to the development of sustainable, high-performance biomaterials for medical applications.

#### 2 Materials and methods

#### 2.1 Materials

The matrix utilized in this investigation comprised magnesium, nHA, and shellac. Magnesium served as the principal matrix material, with nHA-coated shellac employed as an inorganic filler possessing constituents similar to bones and teeth [11]. CaFs were incorporated as a reinforcement in the composite. The magnesium powder used in this study had a purity of 98.5% and a particle size of 100 mesh. Detailed properties of the magnesium powder are summarized in Table 1 [12].

The hydroxyapatite (HA) used in this study was synthesized using the precipitation method, as nanoparticles. The nHA had a Ca/P ratio of 1.67 and a purity of 99%. The mechanical properties of nHA are presented in Table 2. Shellac was prepared using a mixture of 96% ethanol and seedlac, sourced from the Shellac Factory owned by Perum Perhutani in Probolinggo, East Java.

The CaFs were supplied by UD, Rami Kencana, Kulon Progo, Indonesia. The fibers were treated by soaking in a

Table 1: Properties of magnesium

Description	Value	Unit
Particle size	0.06-0.3	mm
Melting point	650	°C
Boiling point	1,090	°C
Density	1,738	kg/m³
Elastic modulus	45	GPa

2% NaOH solution for 6 h, followed by thorough washing with clean water. The fibers were then allowed to air dry at 25°C for 3 days. Subsequently, the CaFs were dried in a furnace at 110°C for 45 min [14]. The surface morphology of the fibers was examined using scanning electron microscopy (SEM), and the result is presented in Figure 1 [15]. The contents of the fibers are detailed in Table 3.

#### 2.2 Fiber tensile properties

The tensile strength of CaFs was measured following the ASTM C1557 standard, using a crosshead speed of 5 mm/min. The results ranged from 220.3 to 303.8 MPa [17]. These results are comparable to those reported for fique fibers, which belong to the same Agave plant family, as noted in a recent review of natural fiber composites [18]. The IFSS was determined using a bundle pull-out test with a JTM-UTS510 machine, operating at a crosshead speed of 0.10 mm/min and a 50 kg load cell transducer. The setup specimens are shown in Figure 2. The transverse elastic modulus of CaF was assessed by testing a composite of CaF with polyester resin as the matrix, with fibers oriented transversely. The volume fraction of CaF used was fixed at 12.76%. The dog bone specimens were adopted for the test, as depicted in Figure 3. The polyester-CaF composite was tested in accordance with the ASTM D638 standard [19], with a crosshead speed of 2 mm/min and a 100 kg load cell transducer. The obtained transverse elastic moduli of CaFs were then put into Eq. (1), the inverse rule-of-mixture, as follows:

Table 2: Mechanical properties of nHA [13]

Description	Value	Unit
Melting point	1,100	°C
Density	3.076	g/cm <sup>3</sup>
Fracture toughness	101.34 ± 4	g/cm³ MJ/m³
Compressive strength	74.08 ± 3	MPa
Elastic modulus	86.12 ± 3	GPa

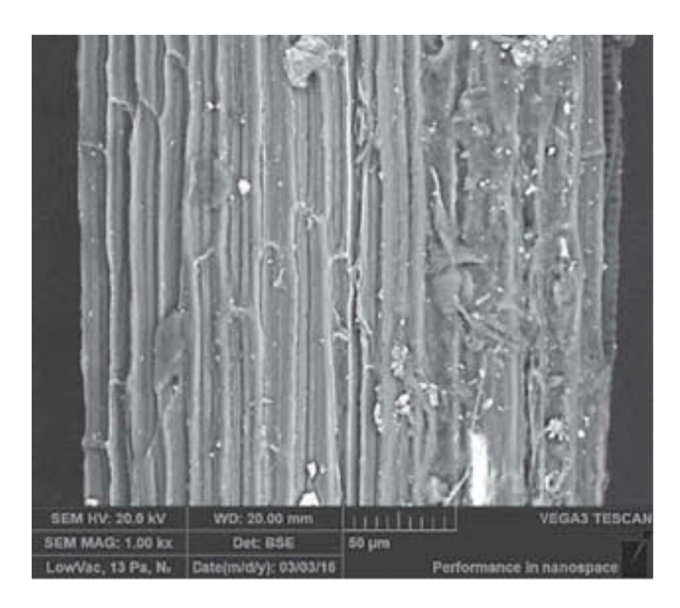


Figure 1: CaF surface.

Table 3: Contents of CaF [16]

Composition	(% by weight)
Hemicellulose	9.45
α-Cellulose	64.23
Lignin	5.91
Ash	4.98
Extracting alcohol-benzene	3.38
Water content alcohol-benzene	11.95

$$1/E_2 = (v_f/E_{f2}) + (v_m/E_m), \tag{1}$$

where  $E_2$ ,  $E_{\rm f2}$ ,  $E_{\rm m}$ ,  $V_{\rm f}$ , and  $V_{\rm m}$  represent, respectively, the transverse modulus of the composite, transverse modulus of a single fiber, modulus of the matrix, volume fraction of the fiber, and volume fraction of the matrix.



Figure 2: IFSS testing setup of specimens.

The deviation between experimental results and prediction models is quantified using Eqs. (2) and (3). Eq. (2) calculates the deviation in the elastic modulus of the composites, while Eq. (3) determines the deviation in their tensile strength.

Elastic modulus deviation (%)  
= 
$$(E_{\text{pred}} - E_{\text{exp}}) \times 100/E_{\text{exp}}$$
, (2)

Tensile strength deviation (%)  
= 
$$(\sigma_{\text{pred}} - \sigma_{\text{exp}}) \times 100/\sigma_{\text{exp}}$$
, (3)

where  $E_{\mathrm{pred}}$ ,  $E_{\mathrm{exp}}$ ,  $\sigma_{\mathrm{pred}}$ , and  $\sigma_{\mathrm{exp}}$  represent the elastic modulus of the prediction result, the elastic modulus of the experimental result, the tensile strength of the prediction result, and the tensile strength of the experimental result, respectively.

#### 2.3 Composite preparation

The CaFs used in this study were subject to alkali treatment by immersion in a 2% sodium hydroxide (NaOH) solution for 6 h. This mercerization process is widely employed to



Figure 3: Dog bone specimens of CaF-polyester.

remove non-cellulosic components such as hemicellulose, lignin, and pectin, thereby improving fiber-matrix adhesion in composite materials [20]. Following treatment, the fibers were thoroughly rinsed with clean water to eliminate any residual NaOH and were subsequently air-dried for 3 days. To further reduce the moisture content, the fibers were ovendried at 110°C for 45 min, a step essential for minimizing residual water that could negatively impact the composite performance [21]. Once dried, the fibers were cut into 10 mm lengths and subjected to mechanical crushing in four cycles using a crusher machine. The crushed fibers were then sieved through a 60 mesh screen to obtain a fine cantula powder suitable for composite reinforcement. The preparation of the Mg/nHA/shellac composite began with the dissolution of one part of nHA in ten parts of shellac solution, continuously stirred at 100°C and 200 rpm for 2 h to ensure homogeneous dispersion. Shellac acts as a natural polymeric binder, improving the stability and uniformity of nHA particles within the composite matrix [22]. The resulting dry powder (30% vol) was subsequently blended with magnesium powder (70% vol) to achieve a homogeneous composite matrix. The composite system was further reinforced by incorporating CaFs at volume fractions of 10, 20, and 30%. All components were thoroughly mixed using a high-speed blender, operating at three different speeds for 1 min each to ensure uniform dispersion. Effective mixing plays a crucial role in achieving homogeneity, directly influencing the mechanical properties of the final composite [23]. The blended mixture was then placed into a mold and compacted under a pressure of 300 MPa. This compaction step facilitated densification and enhanced the mechanical integrity of the green body prior to sintering [24]. The compacted specimens were subsequently removed from the mold and subjected to heat treatment in a furnace at 140°C for 2 h. This thermal processing step promoted better particle bonding and significantly reduced the porosity within the composite which may arise from incomplete wetting of the fibers by the matrix, air entrapment during processing, and fiber degradation [25]. The final composite exhibited a highly dense structure with porosity levels ranging from 0.95 to 2.22% [26]. Experimental studies on natural fiber-reinforced composites indicate that void content beyond a critical threshold (~3-5%) significantly reduces the tensile strength [21].

# 2.4 Tensile testing of Mg/nHA/shellac-CaF composites

The tensile strength and elastic modulus of Mg/nHA/shellac-CaF composites were evaluated according to the

ASTM D638 Type IV standard, employing a 50 kg load cell and a crosshead speed of 2 mm/min. Five specimens were tested for each volume fraction ( $V_{\rm f}$ ) variation of CaF, which are 0, 10, 20, and 30%. The average tensile strength–elongation curves derived from these five replicates are presented in Figure 4. Measurement uncertainty in the tensile test was assessed using standard deviation to quantify the variability of the measured tensile properties for each composition.

Figure 4 shows that the early-stage mechanical behavior underscores the essential role of magnesium as a lightweight and biodegradable matrix material. Magnesium-based composites are widely recognized for their favorable strength-to-weight ratio and biocompatibility, making them highly suitable for biomedical applications [27]. At 0% fiber content, the composite displays the lowest tensile strength, approximately 2.73 MPa, indicating that the unreinforced Mg-HA matrix lacks the structural integrity to sustain higher loads and does not exhibit significant strain-hardening behavior. With the addition of 10% vol. CaF, the tensile strength increases to about 5.48 MPa, reflecting improved stress distribution and enhanced resistance to deformation due to fiber reinforcement. When the fiber content is increased to 20% vol., the tensile strength increases further to approximately 6.96 MPa, suggesting that the fiber-matrix interaction is more effective at this composition, contributing positively to both strength and ductility. At 30% vol. fiber content, the tensile strength exceeds 7.86 MPa. However, this increase is no longer proportional to the added fiber volume, possibly due to microstructural inconsistencies such as fiber agglomeration or

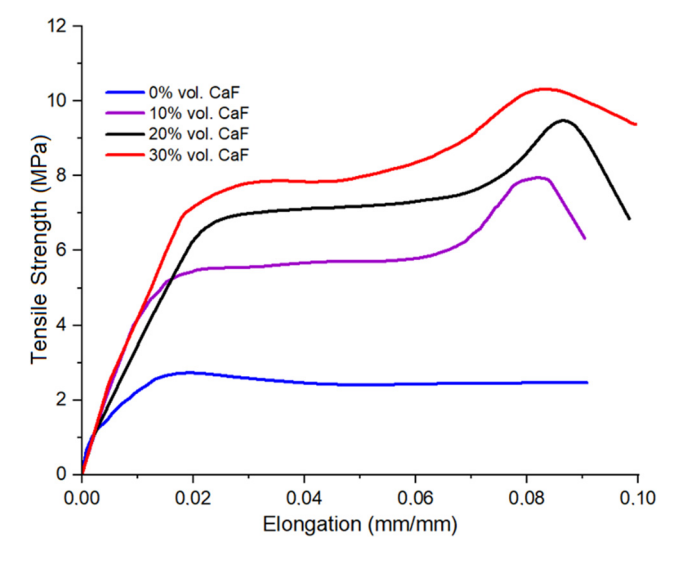


**Figure 4:** Tensile strength–elongation curves of Mg/nHA/shellac matrix composites reinforced with CaFs at various volume fractions.

insufficient fiber-matrix adhesion [28]. Incorporation of natural fibers into composites often promotes the development of porous microstructures, primarily due to the limited interfacial compatibility between the two phases. These interfacial voids can compromise stress transfer efficiency, particularly when the fiber content exceeds the optimal threshold, thereby reducing the overall mechanical performance of the composite [29].

#### 2.5 Brief explanation of selected models

Micromechanical modeling plays a pivotal role in predicting the tensile strength of fiber-reinforced composites, particularly those incorporating natural fibers. Among the various models, the Bowyer-Bader and Hirsch approaches have been extensively utilized due to their effectiveness in capturing the complexities of fiber-matrix interactions. The Bowyer-Bader model offers a semi-empirical framework tailored for composites reinforced with short, discontinuous fibers [30]. It accounts for the contributions of fibers that are both above and below the critical length. considering mechanisms such as fiber fracture and pullout. By segmenting the composite into discrete elements, the model evaluates the overall tensile strength based on factors like fiber length distribution, orientation, and volume fraction. This approach has been effectively applied in various studies to predict the tensile properties of natural fiber composites. For instance, research on lowdensity polyethylene composites reinforced with zalacca fibers demonstrated that the Bowyer-Bader model could accurately predict tensile strength across different fiber volume fractions, highlighting its applicability in natural fiber systems. Another micromechanical approach, the Hirsch model, combines the iso-strain and iso-stress assumptions to estimate the tensile modulus of composite materials [31]. Although originally developed for stiffness prediction, the model has also been adapted to approximate tensile strength. A key feature of the Hirsch model is the introduction of an empirical parameter that characterizes the load-sharing behavior between the fiber and matrix phases. This parameter enables interpolation between the theoretical upper and lower bounds of composite stiffness, resulting in a more refined prediction of mechanical behavior. The model has been employed in several studies to evaluate the tensile performance of fiber-reinforced composites with varying reinforcement contents. For instance, in investigations involving polypropylene matrices reinforced with natural fibers, the Hirsch model was found to yield tensile strength estimations that correlated well with experimental observations [32].

The mechanical behavior of composite materials has also been extensively studied using various modeling approaches that predict stiffness, stress transfer, and failure mechanisms. The Cox-Krenchel model extends the rule of mixtures by incorporating efficiency factors to account for the influence of short fiber length and orientation on load transfer, making it essential for designing injection-molded composite parts [33,34]. In contrast, the Cox model, based on shear-lag theory, describes the stress transfer mechanism between the fiber and matrix in discontinuous fiber-reinforced composites, highlighting the inefficiencies of short fibers due to premature stress relaxation. For laminated composites, the Tsai-Pagano model, derived from classical laminate theory (CLT), provides a fundamental framework for predicting in-plane stiffness and stress distributions across multiple fiber orientations, enabling the design of anisotropic materials with optimized mechanical performance [35,36]. Failure prediction in composites has been extensively addressed through models such as Christensen failure theory, which differentiates between brittle and ductile failure modes in polymer-matrix systems and offers a simplified alternative to more complex tensor-based failure criteria [35]. Expanding on these concepts, the Manera model introduces a micromechanical damage evolution framework that accounts for progressive failure mechanisms, including micro-cracking, fiber pull-out, and delamination, thereby improving the accuracy of composite fatigue life predictions [37,38]. These modeling approaches collectively enable the optimization of composite material design, making them indispensable in high-performance applications such as aerospace, automotive, and structural engineering.

#### 3 Results and discussion

# 3.1 Properties of Mg/nHA/shellac and a single CaF

The properties of Mg/nHA/shellac are presented in Table 4. The transverse strength properties of CaF can be determined using Eq. (1). The tensile strength values for composites with 90° fiber orientation are shown in Table 5. The fiber transverse elastic modulus  $(E_{f2})$  was obtained by orienting CaFs transversely in a polyester-matrix composite, yielding a value of 217 MPa. In comparison, according to the research by Fathoni et al., the fiber longitudinal elastic modulus ( $E_{f1}$ ) for CaF is 3.081 GPa [17]. The

6 — Heru Sukanto et al. DE GRUYTER

**Table 4:** Properties of the Mg/nHA/shellac composite matrix and interactions with the CaF

Description	Value	Unit
Density $(\delta_{\rm m})$	1.56	g/cm³
Porosity $(\phi)$	0.95	%
Tensile strength ( $\sigma_{\rm m}$ )	2.73	MPa
Elastic modulus (E <sub>m</sub> )	32.22	GPa
IFSS between the matrix and CaF ( $\tau_{IFSS}$ )	3.39	MPa
Critical length of the CaF ( $L_c$ )	15.04	mm

significant difference of both elastic moduli ( $E_{f2}$  and  $E_{f1}$ ) indicates that the single CaF exhibits high anisotropy.

Table 4 also shows the IFSS and critical length ( $L_{\rm c}$ ) of interaction between Mg/nHA/shellac and CaFs, which can be derived using Eqs. (4) and (5), respectively [38].

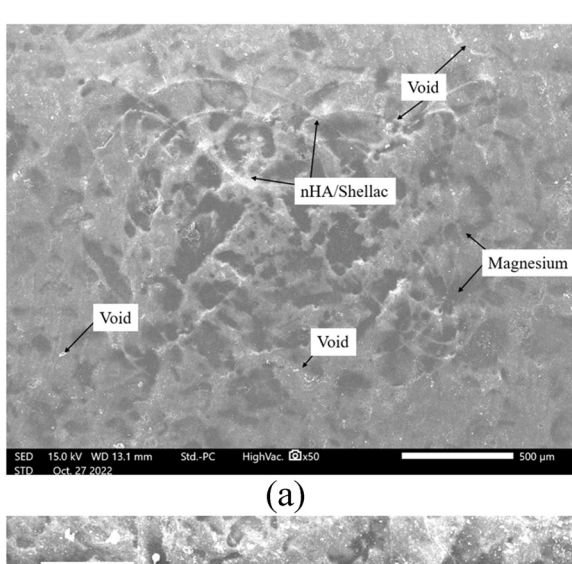
$$\tau_{\rm IFSS} = F/A = F/\pi \cdot d \cdot L,\tag{4}$$

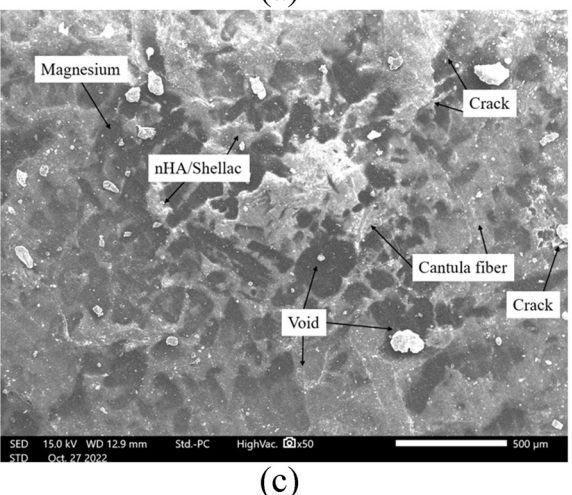
Table 5: Physical and mechanical properties of CaFs

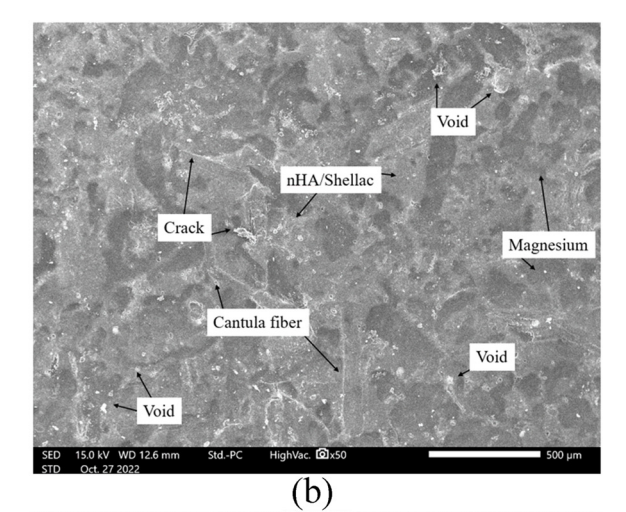
Description	Value	Unit
Diameter (d)	0.15	mm
Density $(\delta_{\rm f})$	1.2	g/cm³
Tensile strength ( $\sigma_{f1}$ )	278	MPa
Elastic modulus (E <sub>f1</sub> )	3.08	GPa
Elongation ( $\varepsilon_{f1}$ )	3.95	(%)
Fiber transverse strength ( $\sigma_{f2}$ )	23.82	MPa
Fiber transverse elastic modulus ( $E_{f2}$ )	217	MPa

$$L_{\rm c} = d\sigma_{\rm f1},\tag{5}$$

where F is the maximum load, A is the interfacial area between the matrix and CaF, L is the length of the fiber embedded in the composite matrix, d is the fiber diameter,  $d\sigma_{\rm fl}$  is the longitudinal tensile strength of fiber, and  $\tau_{\rm IFSS}$  is the IFSS.







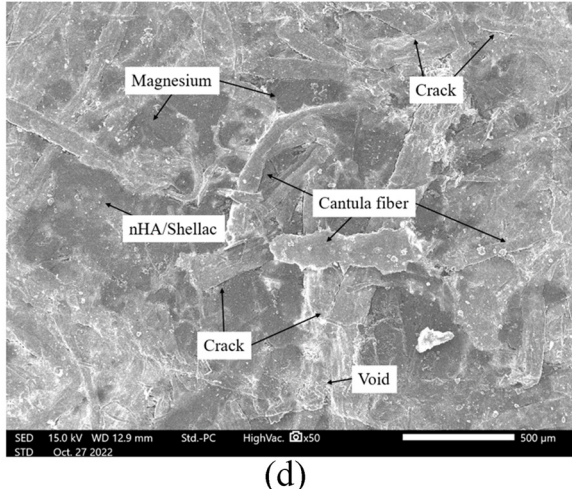


Figure 5: SEM surface images of the Mg/nHA/shellac composite without reinforcement (a) and reinforced with (b) 10%  $V_f$  CaF, (c) 20%  $V_f$  CaF, and (d) 30%  $V_f$  CaF.

The composite surface without reinforcement, shown in Figure 5(a), reveals the presence of magnesium and nHA/ shellac, as well as several voids in the matrix. Figure 5(b) shows the inclusion of CaFs in the composite along with magnesium and nHA/shellac. Several voids and cracks are also visible, indicating imperfect bonding between the fibers and the Mg/ nHA/shellac matrix. Figure 5(c) displays a higher quantity of fibers, allowing for more effective load transfer from the matrix to the fibers. However, there are several cracks and voids caused by the clumping/agglomeration of CaFs, as shellac has not been able to fill the void spaces between the fibers. Further addition of fibers up to 30% V<sub>f</sub> CaF, as shown in Figure 5(d), leads to increased load transfer by the matrix due to the higher content of CaFs in the composite.

Overall, the microstructural analysis of the Mg/nHA/ shellac composite reinforced with CaFs, as shown in Figure 5, reveals the presence of voids, fiber pull-out, and microcracks. These features suggest incomplete interfacial bonding, which can affect the composite's mechanical properties. Similar observations have been reported in previous studies on natural fiber-reinforced biocomposites [25]. A comparable composite system incorporating nHA, magnesium, and shellac with CaF reinforcement exhibited fiber debonding and crack propagation, particularly at higher fiber loadings. These defects were attributed to insufficient fiber wetting and weak matrix-fiber adhesion, which are consistent with the findings in the present study. A related study on agave CaFreinforced HA/shellac composites further supports these results [14]. The study demonstrated that microstructural uniformity plays a key role in enhancing the mechanical strength. However, SEM analysis also highlighted matrixrich regions and fiber clustering, similar to the patterns observed in Figure 5 of this study. The clustering of fibers can lead to stress concentrations, which in turn compromise load transfer efficiency. Improving fiber dispersion and modifying the fiber-matrix interface through surface treatments may help mitigate such issues and improve composite performance. In addition to microstructural concerns, the degradation behavior of magnesium-based materials in biomedical applications has been extensively examined [39]. Research indicates that surface irregularities, including porosity and microcracks, accelerate material degradation in physiological environments. Given that Figure 5 reveals voids and fibermatrix separation, it is likely that these defects could influence the long-term stability of the composite, particularly in applications where biodegradability and corrosion resistance are critical. Meanwhile, studies on shellac's adhesion properties suggest that improving its compatibility with different substrates could minimize defects at the interface [40]. These findings reinforce the idea that modifying the shellac phase in the Mg/nHA composite may enhance its mechanical durability.

The SEM findings from this study align with existing literature reports, confirming that fiber-matrix interactions, void formation, and surface irregularities significantly influence the structural integrity of Mg/nHA/shellac composites.

### 3.2 Prediction of tensile strength of composites

The mathematical models utilized in this study, Hirsch's model and Bowver-Bader's model, have been extensively applied in prior research due to their demonstrated accuracy in predicting the tensile strength of randomly oriented Mg/nHA/shellac-CaF composites across various volume fractions ( $V_f$ ). The initial model employed in this study was Hirsch's model [41], which integrates both parallel and serial rule-of-mixture concepts. Eq. (6) presents Hirsch's model formulation.

$$\sigma_{c} = \chi(\sigma_{m} \cdot V_{m} + \sigma_{f} \cdot V_{f}) + (1 - \chi)((\sigma_{m} \cdot \sigma_{f}))$$

$$/(\sigma_{m} \cdot V_{f} + \sigma_{f} \cdot V_{m})),$$
(6)

where  $\sigma_c$ ,  $\sigma_m$ , and  $\sigma_f$  denote the tensile strength of the composite, matrix, and fiber, respectively. The parameter x determines the stress transfer between the matrix and fibers. Based on the compatibility of experimental and theoretical values, x is determined to be 0.1 for composites with randomly oriented fibers [42].

The second model used was the Bowver-Bader model. which is based on the assumption that the tensile strength of a thermoplastic-matrix composite with short fiber reinforcement is a sum of its subcritical and supercritical fiber and matrix contributions. The tensile strength of the composite ( $\sigma_c$ ) can be derived as follows:

$$\sigma_{\rm c} = \sigma_{\rm f} K_1 K_2 V_{\rm f} + \sigma_{\rm m} \cdot V_{\rm m}, \tag{7}$$

where  $\sigma_c$ ,  $\sigma_m$ , and  $\sigma_f$  represent the tensile strength of the composite, matrix, and fiber, respectively.  $V_{\rm f}$  is the fiber volume fraction,  $V_{\rm m}$  is the matrix volume fraction,  $K_1$  is the fiber orientation factor, and  $K_2$  is the factor related to fiber length. For fibers with  $L > L_c$ ,  $K_2$  is given by

$$K_2 = (L - L_c)/2L.$$
 (8)

For fibers with  $L < L_c$ ,  $K_2$  is given by

$$K_2 = L/2L_c. (9)$$

For random-oriented fiber composites, the value of  $K_1$ is 0.2, based on previous research [43].

The tensile strength of nHA/shellac/Mg-CaF composites predicted by the Hirsch and Bowyer-Bader models is depicted in Figure 6. The Hirsch model notably predicts 8 — Heru Sukanto et al. DE GRUYTER

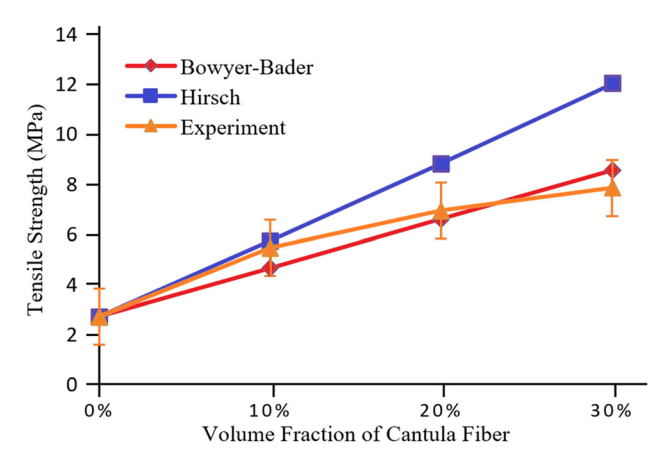


**Figure 6:** Tensile strength of Mg/nHA/shellac-CaF composites: experimental results *versus* Hirsch and Bowyer–Bader models.

significantly higher tensile strengths compared to the Bowyer–Bader model and experimental results across various CaF volume fractions. According to Table 6, the Hirsch model's predicted tensile strength consistently exceeded the experimental values at each volume fraction variation, showing deviations of 0, 5.06, 26.98, and 52.98%, respectively, from the experimental results.

In the prediction using Hirsch's model, the high deviation is attributed to the presence of an inverse rule-of-mixture and the absence of fiber length factors that influence the prediction results. Hirsch's model only considers the stress transfer between the matrix and fibers, represented by the parameter x, with a value of 0.1 for composites with randomly oriented fibers. Consequently, there is a significant increase in the predicted of tensile strength for each volume fraction variation compared to the experimental results.

The results of Bowyer–Bader model were relatively closer to the actual experimental results, as shown in Table 6. For volume fraction variations from 0 to 20%, a negative deviation was observed, as the experimental

**Table 6:** Deviation percentage of tensile strength and elastic modulus between experiment and prediction models

Deviation percentage (%)					
Volume fract	ion (%)	0	10	20	30
Tensile	Hirsch	0	5.06	26.98	52.98
strength	Bowyer-Bader	0	-14.61	-4.91	8.97
Elastic	Cox-Krenchel	0	-9.04	-21.61	-22.38
modulus	Tsai-Pagano	0	29.89	34.17	31.39
	Cox (2D)	-100	179.61	315.37	353.69
	Christensen	0	281.06	400.93	425.93
	Manera	0	19197.11	28508.72	31126.92

results curve was above the prediction curve of the Bowyer-Bader model. Conversely, for the 30% volume fraction variation, a positive deviation was noted, with the experimental result curve falling below the prediction curve of the Bowyer-Bader model. This model includes the parameters  $K_1$  (orientation factor) and  $K_2$  (fiber length factor). For random fiber orientation, the  $K_1$  factor is 0.2, and the  $K_2$  factor depends on the fiber length (L) and the critical fiber length ( $L_c$ ), which was determined to be 0.39. The product of factors  $K_1$  and  $K_2$  yields values smaller than 0.1. Factors influencing more accurate results for Bowyer-Bader model predictions include the orientation factor  $K_1$ and the fiber length factor  $K_2$ . Meanwhile, the Hirsch model relies solely on the stress transfer parameter between the matrix and fiber (x) with a value of 0.1, which is analogous to  $K_1$ . Additionally, the factor (1 - x), multiplied by the inverse rule-of-mixture in the Hirsch model, affects the increase in the predicted value of tensile strength compared to that obtained using the Bowyer - Bader model.

The results demonstrate that Hirsch's model consistently overestimates the tensile strength, while the Bowyer-Bader model provides values that more closely match the experimental data. The deviation in Hirsch's predictions can be attributed to the absence of fiber length considerations and the reliance on an inverse rule-of-mixture, which does not fully capture the load transfer behavior of short fiber composites. Similar findings have been reported in studies of natural fiber-reinforced composites, where the Rule of Mixtures and Hirsch's model tend to overpredict mechanical properties due to their simplified assumptions about stress distribution [44]. The Bowyer-Bader model, which incorporates fiber length  $(K_2)$  and orientation  $(K_1)$  factors, offers better agreement with experimental results. This trend is consistent with findings that demonstrate that the fiber length significantly influences the mechanical properties of short fiber composites [45]. Studies have highlighted that micromechanical models incorporating orientation and aspect ratio adjustments yield more accurate predictions, especially for composites with randomly distributed fibers. Furthermore, models accounting for imperfect bonding conditions, such as fiber waviness and interfacial debonding, tend to provide better estimations than purely theoretical models like Hirsch's approach [46]. The experimental results also suggest that increasing fiber content beyond a certain threshold affects the accuracy of both models. At higher fiber volume fractions (30%), the Bowyer-Bader model slightly overestimated the tensile strength, while Hirsch's model continued to show significant deviations. This aligns with research indicating that fiber clustering at higher loadings leads to stress concentrations, reducing the overall tensile strength [47]. The findings further indicate that void formation and matrix-fiber

adhesion must be considered in micromechanical models to improve the predictive accuracy. In this regard, incorporating empirical correction factors has been suggested to account for fiber agglomeration effects in natural fiber-reinforced composites [48]. Overall, the comparison with previous studies confirms that while Hirsch's model provides a theoretical upper bound, the Bowyer-Bader model remains a more practical tool for predicting the tensile strength of Mg/nHA/shellac-CaF composites.

# 3.3 Prediction of the elastic modulus of composites

Four mathematical models were tested to assess the agreement of their elastic modulus calculations with experimental results. The first model, proposed by Halpin-Tsai and Pagano, was used to estimate the elastic modulus of composites reinforced by randomly oriented fibers. The model is mathematically represented by Eq. (10) [49].

$$E_{\rm c} = 0.325E_1 + 0.625E_2,$$
 (10)

where  $E_c$ ,  $E_1$ , and  $E_2$  represent the elastic modulus of randomly oriented fibers, longitudinal orientation, and transverse orientation, respectively. These elastic moduli are clarified for similar aspect ratios (L/d) and volume fraction  $(V_{\rm f})$ . The Halpin-Tsai model was also used to determine both  $E_1$  and  $E_2$ , as shown in Eqs. (11) and (12).

$$\begin{split} E_1 &= E_{\rm m}((1+2(L/d)\eta_1\cdot V_{\rm f})/(1-\eta_1\cdot V_{\rm f})),\\ \eta_1 &= (E_{\rm fl}/E_{\rm m})-1)/((E_{\rm fl}/E_{\rm m})+2(L/d)), \end{split} \tag{11}$$

$$E_2 = E_{\rm m} ((1 + 2\eta_2 V_{\rm f})/(1 - \eta_2 V_{\rm f})),$$
  

$$\eta_2 = ((E_{\rm f2}/E_{\rm m}) - 1)/((E_{\rm f2}/E_{\rm m}) + 2(L/d)),$$
(12)

where  $E_{f1}$ ,  $E_{f2}$ , and  $E_{m}$  represent the corresponding longitudinal modulus of the fiber, the transverse modulus of the fiber, and the elastic modulus of matrix, respectively [43].

The second model used to predict the elastic modulus was the Cox-Krenchel model. Based on the calculation of the dimension and orientation factors of the fiber phase [50], the elastic modulus of the composite in the Cox-Krenchel model can be derived as follows [51]:

$$E_{\rm c} = \eta_1 \, \eta_0 \, E_{\rm f} \, V_{\rm f} + E_{\rm m} \, V_{\rm m}. \tag{13}$$

In this equation,  $\eta_1$  and  $\eta_0$  represent the fiber length distribution and orientation factors, respectively. In the Cox-Krenchel model, the presence of voids can be ignored. The fiber orientation factor is expressed as [42]

$$\eta_0 = \cos^4(\alpha_0),\tag{14}$$

where  $\alpha_0$  is the limiting angle of fiber orientation. For inplane random fiber orientation laminates, the orientation factor ( $\alpha_0$ ) was 0.375 according to Thomason *et al.* [52]. The value of  $\eta_1$  was calculated based on Cox's shear lag theory, given by [53]

$$\eta_1 = 1 - (\tan h(\beta L/2))/(\beta L/2),$$
 (15)

$$\beta = 2/d(\text{sqr}[E_{\text{m}}/(E_{\text{fl}}(1 - \nu_{\text{m}}) \ln(\pi/(x_i \cdot V_{\text{f}}))]). \tag{16}$$

In this context,  $\beta$  is the shear parameter, denoting the stress concentration rate coefficient at the end of the fiber, and  $v_{\rm m}$  is the Poisson's ratio of the matrix. For this model, the fiber arrangement was considered rectangular, thus  $x_i = 4$ .

The third model was Christensen model, based on the behavior of a composite system with a two-dimensional random fiber orientation. This model considered the effect of fiber orientation and fiber-matrix interaction, which are shown in the following equation [54]:

$$E_{\rm c} = 0.3 V_{\rm f} E_{\rm f} + 0.3(1 - V_{\rm f}) E_{\rm m} + 0.7 E_{\rm m} [(E_{\rm f}(1 + V_{\rm f}) + E_{\rm m}(1 - V_{\rm f}))/(E_{\rm f}(1 - V_{\rm f}) + E_{\rm m}(1 + V_{\rm f}))].$$
(17)

Manera proposed an empirical simplification of the Christensen model, as shown in Eq. (18). The Manera model assumes that the mechanical properties of a randomly oriented fiber in the composite are equivalent to those of laminates with an infinite number of layers oriented in any direction.

$$E_{\rm c} = V_{\rm f}(0.36E_{\rm fl} + 2E_{\rm m}) + 0.89E_{\rm m}.$$
 (18)

The fourth model utilized is the Cox model, which represents paper as a planar mat of continuous fibers without matrix material. This model is the simplest compared to the others. Cox introduced the concept of averaging the elastic constants over all possible orientations by integration. This model is divided into two equations: the first one for the 2D case, applicable when the fiber length is greater than the thickness of the part, as shown in Eq. (19), and the second one for the 3D case, applicable when the fiber length is less than the thickness of the part, as shown in Eq. (20) [49].

$$E_{\rm c} = (E_{\rm f} \ v_{\rm f})/3,$$
 (19)

$$E_{\rm c} = (E_{\rm f} \ v_{\rm f})/6,$$
 (20)

where  $v_f$  is Poisson's ratio of the fiber.

Figure 7 shows that the predictions of the Tsai-Pagano model closely match the experimental results compared to other models. The Tsai-Pagano model demonstrates predictive values for elastic modulus, as also shown in Table 6, with successive deviations of 0, 29.89, 34.17, and 31.39% at  $V_{\rm f}$  variations of 0, 0.1, 0.2, and 0.3, respectively. This model incorporates anisotropic characteristics and aspect ratios of fibers, considering both the longitudinal elastic modulus ( $E_{\rm fl}$ ) and transverse elastic modulus ( $E_{\rm f2}$ ) of individual CaFs to determine the elastic moduli of longitudinal and transverse composites. Fortunately, both values are known:  $E_{\rm fl}=3.081\,{\rm GPa}$  according to previous research [17] and  $E_{\rm f2}=0.217\,{\rm GPa}$  based on the test results of this study.

Referring to the calculation results shown in Table 6, the predictions of the Cox-Krenchel model are the closest to the experimental results, with a maximum deviation of 22.38% at a  $V_{\rm f}$  of 30%. The Cox-Krenchel model has a small deviation from the experimental results because it accounts for the fiber orientation factor  $(\eta_0)$ , the fiber length distribution ( $\eta_1$ ), the stress concentration coefficient at the fiber end  $(\beta)$ , and Poisson's ratio of the matrix. The prediction of the elastic modulus obtained with the Christensen model shows the greatest deviation, exceeding the experimental results for all  $V_f$ s. This is because the Christensen model relies only on the values of the elastic modulus of the matrix and volume fraction, without considering the effects of fiber orientation and matrix-fiber interaction. The results of the Christensen model are also commensurate with those of the Monera model, because the nHA/Mg/shellac matrix and CaFs do not meet the model's requirements, such as an  $E_{\rm m}$  ranging from 2 to 4 GPa and a high fiber aspect ratio (L/d > 300) [43]. In this study,  $E_{\rm m}$  was 32.22 MPa. In the Cox model (2D), the predicted results are significantly different from the experimental results because this model only assumes paper as a planar mat of continuous fibers without matrix material and concludes that fiber orientation is more important than the fiber length. However, the Cox model is the simplest for

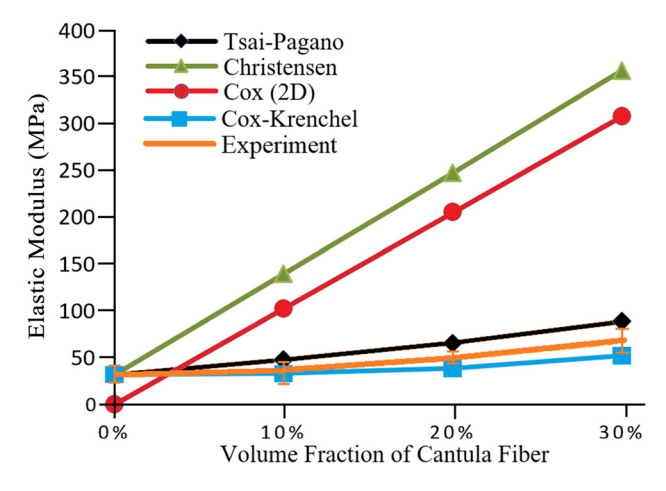


**Figure 7:** Elastic modulus of Mg/nHA/shellac-CaF composites modeled by Tsai-Pagano, Cox-Krenchel, Christensen, Cox (2D), and Manera.

predicting the elastic modulus compared to the other three models.

None of these elastic modulus models could accurately predict results similar to those obtained experimentally, which could be attributed to the exclusion of critical length and interfacial strength factors in the equations, as demonstrated by the Bowyer-Bader model in the tensile strength prediction equation. The advantage of the Cox-Krenchel model over other models lies in its consideration of the length distribution and orientation of the fibers. The advantage of the Tsai-Pagano model is that it incorporates the aspect ratio and the transverse elastic modulus of the fibers in its equations to obtain the longitudinal and transverse elastic moduli of composites. The Cox (2D) model is based on the elastic modulus of fibers without considering the matrix material. The Monera model prediction only calculates the longitudinal modulus of fibers, while the Christensen model considers only the effects of fiber orientation and fiber-matrix interaction.

Despite demonstrating high accuracy at a lower fiber content, the Tsai-Pagano model exhibited increasing deviations as the fiber volume fraction  $(V_f)$  increased, suggesting that fiber agglomeration and interfacial debonding significantly influence the effective stiffness of the composite. This trend aligns with previous findings, indicating that beyond a critical fiber loading, elastic modulus predictions tend to diverge due to clustering effects and stress concentrations [47]. The Cox-Krenchel model, which accounts for fiber orientation ( $\eta_0$ ) and fiber length efficiency  $(\eta_1)$ , also showed reasonable agreement with experimental results, with deviations not exceeding 22.38%. This finding is consistent with previous studies, highlighting that micromechanical models incorporating fiber orientation parameters generally yield more accurate stiffness predictions for short-fiber composites [20]. Conversely, the Christensen model exhibited the most substantial deviations from experimental values, as it primarily relies on the matrix modulus and fiber volume fraction while neglecting the fiber orientation and fiber-matrix interactions. A similar discrepancy was observed in previous studies, which found that micromechanical models failing to account for interfacial bonding and fiber orientation tend to overestimate the elastic modulus of biodegradable composites [55]. The Manera model, which simplifies the Christensen approach by assuming an infinite number of fiber orientations, produced comparable deviations, indicating that such assumptions do not hold well for Mg/nHA/ shellac-CaF composites with defined fiber distributions [39].

#### 4 Conclusions

The addition of random oriented CaF to the Mg/nHA/ shellac matrix resulted in increased tensile strength and elastic modulus. The transverse modulus  $(E_{f2})$  of a single CaF was obtained by tensile testing using polyester resin and CaF in the transverse direction with definite  $V_{\rm f}$  in the inverse rule-of-mixture. Hence, CaF is anisotropic with  $E_{f1}$ and  $E_{\rm f2}$  values of 3.081 and 0.217 GPa, respectively. A comparison of the tensile strength between the experimental method and the micromechanical prediction model shows that Bowver-Bader's model provided good prediction on composites. Meanwhile, the comparative study of elastic modulus prediction between the experimental method and a few of selected models showed that Cox-Krenchel's model resulted in the best prediction of elastic modulus.

Future research should prioritize the development of biocompatible isotropic fibers as reinforcements for the Mg/nHA/shellac matrix system. The significant deviation observed between experimental tensile results and micromechanical model predictions, particularly in higher fiber volume fractions, is believed to be largely attributed to the anisotropic nature and irregular distribution of CaFs. These characteristics may lead to uneven stress transfer, local fiber agglomeration, and variable interfacial adhesion, which cannot be fully captured by conventional modeling approaches. Moreover, addressing other sources of variability is equally crucial. For instance, inconsistency in fiber surface treatment (e.g., level of cleaning, drying, or chemical modification) and variations in matrix processing conditions (such as curing time, mixing uniformity, and temperature control) can lead to structural heterogeneity and porosity, ultimately affecting the mechanical performance. Standardizing these parameters or introducing more refined processing protocols may improve the reproducibility and alignment between theoretical predictions and actual performance. To advance predictive accuracy and material reliability, future work should incorporate multiscale modeling techniques that consider fiber morphology, orientation, and interfacial properties, complemented by experimental validation. Such integrated approaches will provide deeper insights into the structureproperty relationships and enable more precise optimization of natural fiber-reinforced biocomposites for biomedical or structural applications.

Acknowledgments: This work was funded by the Hibah Group Research of Sebelas Maret University, Surakarta, with contract number: 194.2/UN27.22/PT.01.03/2024.

Funding information: This work was funded by the Hibah Group Research of Sebelas Maret University, Surakarta, with contract number: 194.2/UN27.22/PT.01.03/2024.

Author contributions: Heru Sukanto: conceptualization, original draft review, and supervision. Joko Triyono: methodology and project supervision. Dody Ariawan: methodology and writing - review. Wijang Wisnu Raharjo: resources and experimental expertise. Muhammad Takbir Alfarisi: experimental data acquisition and supervision. Rachmad Imbang Tritjahjono: data analysis and experiment supervision. Latifah Nur Hikmah: project administration. All authors have accepted responsibility for the entire content of this manuscript and approved its submission.

Conflict of interest: The authors state no conflict of interest.

Data availability statement: All data generated or analyzed during this study are included in this published

#### References

- Purnaning D, Taufik A, Zulkarnaen DA. Penyuluhan Penanganan Tepat Kasus Patah Tulang Pada Masyarakat Di Desa Senggigi. Proceeding of Seminar Nasional Pengabdian kepada Masyarakat (Pepadu), Vol. 2, 2020, p. 129-32 Indonesian.
- Azharul F. Dharmanto A. Wilarso D. Penguijan Sifat Mekanik Implan [2] Plate Dan Sekrup Fiksasi Internal Tulang Femur Dari Material Hidroksiapatit Bovine Dan Polimer Biodegradasi Menggunakan Printer 3D. Traksi: Maj Ilm Tek Mesin. 2020;20:45-58 Indonesian.
- Gunawarman G, Affi J, Ilhamdi I, Nuswantoro NF, Tjong DH, [3] Manjas M. Kontribusi Lapisan Hidroksiapatit pada Purwarupa Implan Titanium terhadap Nilai Osseointegrasi Melalui Removal Torque Test. JMPM. 2022 Mar;5(2):91-9 Indonesian [cited 2024 Sep 14] https://journal.umy.ac.id/index.php/jmpm/article/view/13904.
- Zhou H, Liang B, Jiang H, Deng Z, Yu K. Magnesium-based biomaterials as emerging agents for bone repair and regeneration: from mechanism to application. J Magnes Alloy. 2021;9:779-804.
- Warburton A, Girdler SJ, Mikhail CM, Ahn A, Cho SK. Biomaterials in [5] spinal implants: A review. Neurospine. 2020;17:101-10.
- Venkatarajan S, Subbu C, Athijayamani A, Muthuraja R. Mechanical properties of natural cellulose fibers reinforced polymer composites - 2015-2020: A review. Mater Today. 2021;47:1017-24.
- [7] Garkhail SK. Mechanical properties of natural-fibre-mat-reinforced thermoplastics based on flax fibres and polypropylene. Appl Compos Mater. 2000;7:351-72.
- [8] Pratama R, Jalinus N, Sari NR, Arafat A, Implant B. Analisis Struktur Dan Fase Paduan Seng Mampu Terserap Tubuh Untuk Aplikasi Implan Biomedis. Ranah Res. 2019;798-804 Indonesian.

- Raharjo WP, Soenoko R, Purnowidodo A, Choiron MA. Experimental and micromechanical modelling of randomly oriented zalacca fibre/low-density polyethylene composites fabricated by hotpressing method. Cogent Eng. 2018;5:1518966.
- [10] Alam N, Ambardi P, Prajitno DH. Pengaruh Perlakuan Pelarutan Terhadap Sifat Mekanik dan Strukturmikro Paduan TernerZr-Nb-Mo Untuk Biomaterial. | Ind Tech Ass. 2019;13:15-22 Indonesian.
- [11] Khoirivah M. Cahvaningrum SE. Sintesis Dan Karakterisasi Bone Graft Dari Komposit Hidroksiapatit/Kolagen/Kitosan (Ha/Coll/Chi) Dengan Metode Ex-Situ Sebagai Kandidat Implan Tulangsynthesis and Characteritation of Bone Graft From Hydroxyapatite/Collagen/ Chitosan (Ha/Coll/Chi) Composite. Indones J Chem. 2018;7:25-9
- [12] Kumar K. Gill RS. Batra U. Challenges and opportunities for biodegradable magnesium alloy implants. Mater Technol. 2018:33:153-72.
- [13] Mahfudi I, Triyono J, Triyono T. Karakterisasi biokomposit sheep hydroxyapatite (sha)/shellac/tepung terigu. Mekanika: Maj Ilm Mekanika. 2019;17:44-8 Indonesian.
- [14] Rahardjo WW, Pujiyanto E, Saputro BA, Majid A, Triyono J. Agave Cantula fiber-reinforced biocomposites of hydroxyapatite/shellac as a dental material. J Nat Fibers. 2022;19:13012-24.
- [15] Ubaidillah U, Raharjo WW, Wibowo A, Harjana H, Mazlan SA. Influence of additional coupling agent on the mechanical properties of polyester-Agave cantala roxb based composites. Proceeding of the 4th International Conference and Exhibition on Sustainable Energy and Advanced Materials. Vol. 1717, No. 1 2015. p. 040021.
- [16] Ramadhan MRB, Salim MS, Fanani E, Ariawan D, Surojo E. Effect of alkaline treatment and fumigation (fumigation) on the mechanical properties of fiber unsaturated polyester-cantula composite with compression molding method. Mekanika: Maj Ilm Mekanika. 2022;21:40-4 Indonesian.
- [17] Fathoni A, Raharjo WW, Triyono T. Pengaruh Perlakuan Panas Serat Terhadap Sifat Tarik Serat Tunggal dan Komposit Cantula-rHDPE. Simetris: J Tek Mesin Elektro Ilm Komput. 2017;8:67-74 Indonesian.
- [18] Gómez SA, Córdoba E. Composite materials reinforced with figue fibers - a review. Rev Uis Ing. 2022;21:163-78.
- [19] ASTM International. ASTM D638-14, Standard test method for tensile properties of plastics [internet]. Vol. 82, 2015 Apr. p. 1-15. [cited 2024 Aug. 12]. http://repositorio.usek.edu.ec/bitstream/ 123456789/2628/1/ASTM%20D638-14.pdf.
- [20] Kabir MM, Wang H, Lau KT, Cardona F. Chemical treatments on plant-based natural fibre reinforced polymer composites: An overview. Compos B Eng. 2012;43:2883-92.
- [21] Pickering KL, Efendy MGA, Le TM. A review of recent developments in natural fibre composites and their mechanical performance. Compos -A: Appl Sci Manuf. 2016;83:98-112.
- [22] Thombare N, Kumar S, Kumari U, Sakare P, Yogi RK, Prasad N, et al. Shellac as a multifunctional biopolymer: A review on properties, applications and future potential. Int J Biol Macromol. 2022;215:203-23.
- [23] Alsuwait RB, Souiyah M, Momohjimoh I, Ganiyu SA, Bakare AO. Recent development in the processing, properties, and applications of epoxy-based natural fiber polymer biocomposites. Polymers. 2022;15:145.
- [24] Yallew TB, Kassegn E, Aregawi S, Gebresias A. Study on effect of process parameters on tensile properties of compression molded natural fiber reinforced polymer composites. SN Appl Sci. 2020;2:338.

- [25] Utami DP, Triyono J, Raharjo WW, Tritjahjono RI. Analisys of tensile strength, wear rate, and cristallinity of biocomposite nano-HA/ magnesium/shellac reinforced cantula fiber for bone screw material. Mekanika: Maj Ilm Mekanika. 2024;23:75.
- [26] Wibowo Y. Analisa Pengujian Bending, Ketangguhan Retak dan Laju Biodegradasi Biokomposit Nano-Ha/Magnesium/Shellac yang Diperkuat Serat Cantula Untuk Material Sekrup Tulang. Thesis. Universitas Sebelas Maret: 2018 Indonesian.
- [27] Sabet A, Jabbari A, Sedighi M. Microstructural properties and mechanical behavior of magnesium/hydroxyapatite biocomposite under static and high cycle fatigue loading. J Compos Mater. 2018;52:1711-22.
- [28] Tran LQN, Yuan XW, Bhattacharyya D, Fuentes C, Van Vuure AW, Verpoest I. Fiber-matrix interfacial adhesion in natural fiber composites. Int | Mod Phys B. 2015;29:1540018.
- [29] Figueroa V, Diaz-Vidal T, Cisneros-López EO, Robledo-Ortiz JR, López-Naranjo EJ, Ortega-Gudiño P, et al. Mechanical and physicochemical properties of 3D-printed agave fibers/poly(lactic) acid biocomposites. Materials. 2021;14:3111.
- [30] Bowyer WH, Bader MG. On the re-inforcement of thermoplastics by imperfectly aligned discontinuous fibres. J Mater Sci. 1972;7:1315-21.
- [31] Hirsch TJ. The effects of the elastic moduli of the cement paste matrix and aggregate on the modulus of elasticity of concrete. Dissertation. Agricultural and Mechanical College of Texas; 1961.
- Popovics S, Erdey MRA. Estimation of the modulus of elasticity of concrete-like composite materials. Mat Constr. 1970;3:253-60.
- [33] Cox HL. The elasticity and strength of paper and other fibrous materials. Br J Appl Phys. 1952;3:72-9.
- [34] Pant M, Palsule S. Prediction of tensile properties of natural fiber reinforced PP hybrid composites by Facca-Kortschot-Yan (FKY) and palsule equations. J Phys: Conf Ser. 2024;2837:012005.
- [35] Christensen RM. Mechanics of composite materials. 1st edn. Mineoki: Dover: 1979.
- [36] Manera M. Elastic properties of randomly oriented short fiber-glass composites. J Compos Mater. 1977;11:235-47.
- [37] Talreja R. Multi-scale modeling in damage mechanics of composite materials. J Mater Sci. 2006;41:6800-12.
- [38] Liu Y, Ma Y, Yu J, Zhuang J, Wu S, Tong J. Development and characterization of alkali treated abaca fiber reinforced friction composites. Compos Interfaces. 2019;26:67-82.
- [39] Liu L, Gebresellasie K, Collins B, Zhang H, Xu Z, Sankar J, et al. Degradation rates of pure zinc, magnesium, and magnesium alloys measured by volume loss, mass loss, and hydrogen evolution. Appl Sci. 2018;8:1459.
- [40] Wang J, Chen L, He Y. Preparation of environmental friendly coatings based on natural shellac modified by diamine and its applications for copper protection. Prog Org Coat. 2008:62:307-12.
- [41] Hirsch TJ. Modulus of elasticity iof concrete affected by elastic moduli of cement paste matrix and aggregate. J Am Concr Inst. 1962;59:427-52.
- [42] Andre NG, Ariawan D, Mohd Ishak ZA. Elastic anisotropy of kenaf fibre and micromechanical modeling of nonwoven kenaf fibre/ epoxy composites. J Reinf Plast Compos. 2016;35:1424-33.
- [43] Ariawan D, Surojo E, Triyono J, Purbayanto IF, Pamungkas AF, Prabowo AR. Micromechanical analysis on tensile properties prediction of discontinuous randomized zalacca fibre/high-density polyethylene composites under critical fibre length. Theor Appl Mech Lett. 2020;10:57-65.

- [44] Fu S, Lauke B. Effects of fiber length and fiber orientation distributions on the tensile strength of short-fiber-reinforced polymers. Compos Sci Technol. 1996;56:1179-90.
- [45] Chauhan V, Kärki T, Varis J. Review of natural fiber-reinforced engineering plastic composites, their applications in the transportation sector and processing techniques. J Thermoplast Compos Mater. 2022;35:1169-209.
- [46] Iskandar ME, Aslani A, Liu H. The effects of nanostructured hydroxyapatite coating on the biodegradation and cytocompatibility of magnesium implants. J Biomed Mater Res. 2013;101A:2340-54.
- [47] Jawaid M, Khalil HPS. Cellulosic/synthetic fibre reinforced polymer hybrid composites: A review. Carbohydr Polym. 2011;86:1-18.
- [48] Pickering KL, Efendy MGA, Le TM. A review of recent developments in natural fibre composites and their mechanical performance. Compos-A: Appl Sci Manuf. 2016;83:98-112.
- [49] Gibson RF. Principles of composite material mechanics. 4 edn. Boca Raton: CRC Press; 2016.

- [50] Pervaiz M, Sain M, Ghosh A. Evaluation of the influence of fibre length and concentration on mechanical performance of hemp fibre reinforced polypropylene composite. J Nat Fibers. 2006;2:67-84.
- Halpin JC. Stiffness and expansion estimates for oriented short [51] fiber composites. J Compos Mater. 1969;3:732-4.
- Thomason JL, Vlug MA, Schipper G, Krikor HGLT. Influence of fibre length and concentration on the properties of glass fibrereinforced polypropylene: Part 3. Strength and strain at failure. Compos-A: Appl Sci Manuf. 1996;27:1075-84.
- [53] Garkhail SK, Heijenrath RWH, Peijs T. Mechanical properties of natural-fibre-mat-reinforced thermoplastics based on flax fibres and polypropylene. Appl Compos Mater. 2000;7:351-72.
- [54] Christensen RM. Asymptotic modulus results for composites containing randomly oriented fibers. Int I Solids Struct, 1976:12:537-44.
- Jaiswal S, Dubey A, Lahiri D. The influence of bioactive [55] hydroxyapatite shape and size on the mechanical and biodegradation behaviour of magnesium based composite. Ceram Int. 2020;46:27205-18.